Effect of Mold Coating Materials and Thickness on Heat Transfer in Permanent Mold Casting of Aluminum Alloys

A. HAMASAIID, M.S. DARGUSCH, C.J. DAVIDSON, S. TOVAR, T. LOULOU, F. REZAÏ-ARIA, and G. DOUR

In permanent mold casting or gravity die casting (GDC) of aluminum alloys, die coating at the casting-mold interface is the most important single factor controlling heat transfer and, hence, it has the greatest influence on the solidification rate and development of microstructure. This investigation studies the influence of coating thickness, coating composition, and alloy composition on the heat transfer at the casting-mold interface. Both graphite and TiO_2-based coatings have been investigated. Two aluminum alloys have been investigated: Al-7Si-0.3Mg and Al-9Si-3Cu. Thermal histories throughout the die wall have been recorded by fine type-K thermocouples. From these measurements, die surface temperatures and heat flux density have been evaluated using an inverse method. Casting surface temperature was measured by infrared pyrometry, and the interfacial heat-transfer coefficient (HTC) has been determined using these combined pieces of information. While the alloy is liquid, the coating material has only a weak influence over heat flow and the thermal contact resistance seems to be governed more by coating porosity and thickness. The HTC decreases as the coating thickness increases. However, as solidification takes place and the HTC decreases, the HTC of graphite coating remains higher than that of ceramic coatings of similar thickness. After the formation of an air gap at the interface, the effect of coating material vanishes. The peak values of HTC and the heat flux density are larger for Al-7Si-0.3Mg than for Al-9Si-3Cu. Consequently, the apparent solidification time of Al-9Si-3Cu is larger than that of Al-7Si-0.3Mg and it increases with coating thickness.

I. INTRODUCTION

IN casting, it is well established that the microstructure of solidified alloys depends on the rate of solidification. In permanent mold casting or gravity die casting (GDC), heat removal from the molten alloy proceeds through a layer of solidified alloy, the casting-mold interface, and then through the die. With a metallic die, heat loss is usually limited by the properties of the casting-mold interface, which is characterized by the roughness of the contacting surfaces and coating properties.

The coatings used in GDC usually have a relatively large thickness: from about 50 to 150 μm. These coatings maintain mechanical integrity and prevent any premature solidification to promote complete filling of the die cavity, and they can be used to control the solidification rate. Furthermore, the coating protects the die from thermal shock by the molten metal and prevents soldering of the die. Regions of die where a slow solidification rate is required, like a feeder, usually have a thicker coating than the part where the solidification rate must be rapid. When a more rapid solidification rate is required, the coating is often changed from ceramic to graphite. These functions of coatings necessitate a low thermal conductivity, to control the heat transfer from the casting to the die, and a good chemical stability, to prevent chemical reaction with the molten metal. The die coating is the thermal barrier that plays a major role on the limitation of heat extraction during casting solidification.

In general, the heat exchange between the casting and the die is characterized by the heat-transfer coefficient (HTC) at the casting-mold interface, which is the inverse of the thermal contact resistance existing at this interface. In GDC, the coating completely separates the die surface from the casting surface. Because its thickness is important, it should be one of the key parameters on which HTC at the interface is based. Knowledge of the HTC is of great benefit for simulating the solidification, modeling the process parameters, and controlling the microstructure of castings.

It is known that a coating offers a resistance to heat transfer due to its lower thermal conductivity. The thermal resistance due to various coatings can be linked

A. HAMASAIID, Ph.D Student, is with CAST CRC, School of Engineering, The University of Queensland, Brisbane QLD, Australia and the Ecole des Mines d'Albi-Carmaux, Université Paul Sabatier, Toulouse, France. Contact e-mail: hamasaii@enstimac.fr M.S. DARGUSCH, Project Leader, is with the CAST CRC, School of Engineering, The University of Queensland, St. Lucia, Brisbane QLD 4072, Australia. C.J. DAVIDSON, Project Leader, is with the CSIRO Manufacturing and Materials Technology, Kenmore, QLD, Australia. S. TOVAR, Technician (Metallurgy, Metallographic), F. REZAÏ-ARIA, Professor, and G. DOUR, Associate Professor, are with the Ecole des Mines d'Albi-Carmaux, CROMeP, 81 013, Albi Cedex 09, France. T. LOULOU, Professor, is with the Institut Universitaire de Technologie de Lorient, 56100, Lorient, France.

to their composition, porosity level, thickness, microstructure, as well as surface roughness and method of application of the coating on the die surface.[1,2,3] Controlling each of these elements independently is difficult, and so it is not clear which of these properties has the most influence on the thermal resistance of coatings. An effort to estimate the effect of a coating on heat transfer requires a close examination of each of the aforementioned properties. Of these properties, both coating thickness and composition will be discussed in the present article.

A few steady-state coating investigations provide a limited understanding of the effect of coating thickness and composition on the heat transfer in GDC. Chiesa[1,4] reports that the HTC for a graphite-coated die is twice that of a ceramic-coated die for the same thickness of coating. However, Sciama and Ribou, Tomasevic, and Davies[5,6,7] conclude that the coating composition has only a minor effect on HTC. More recently, Hallam and Griffith[8] found slight differences in HTC between graphite-based coatings and those based on ceramic. For Jahedi and Giannos,[9] the HTC for a TiO_2-based coating is greater those that of talc or mica coatings. Meanwhile, the authors[1,5–7,10] all agree that the HTC decreases as the coating thickness increases. However, the details of the relationship between HTC and coating thickness are not well understood. In general, the investigators compare the maximum of HTC for different conditions of coating. Because the HTC changes during the course of solidification, a study about the effect of both the coating thickness and the coating composition on heat transfer at the interface should contain not only a maximum of HTC *vs* coating thickness, but also its variation as a function of solidification time.

There are three main purposes of the present work. The first is to devise an experimentally reproducible robust and accurate technique that enables the evaluation of the HTC as a function of time at the casting-mold interface under the conditions similar to those encountered in foundry practice. The second is to further study the effect of coating thickness and coating composition. Finally, we aim at completing the study with the effect of alloy composition on the heat transfer and solidification time during casting solidification in permanent mold casting.

II. EXPERIMENTAL METHOD

A. *Casting Procedure*

The trials were carried out on a die made of X38CrMoV-5 (Eq. AISI H11) steel with the dimensions $210 \times 210 \times 50$ mm, the die cavity having a rectangular shape with dimensions $110 \times 110 \times 20$ mm. The gate system was lateral with a 4-mm-thick gate (Figure 1). The chemical composition of the mold material is shown in Table I.

A pneumatic system controlled both the opening and the closing of the die that could slide along horizontal columns. The parting plane was vertical and Figure 1 shows a top view of the horizontal cross section. In order to measure the temperature in the die and of the casting surface, the fixed part of the die was instrumented with a gage that will be described in the next paragraph, as illustrated in Figure 1. Two kinds of coatings have been used during the tests: a white coating based on TiO_2 and a black coating based on graphite. An established manual spray technique was used to apply the coatings to the surface of the die, which was preheated to about 200 °C to 210 °C. The coating thickness was measured using an Erichsen probe (Mini-Test2100). The alloys investigated during the tests were Al-7Si-0.3Mg and Al-9Si-3Cu. The chemical compositions of the investigated alloys are shown in Table II. The melt temperature was 750 °C. The alloys were poured manually into the die with a preheated ladle.

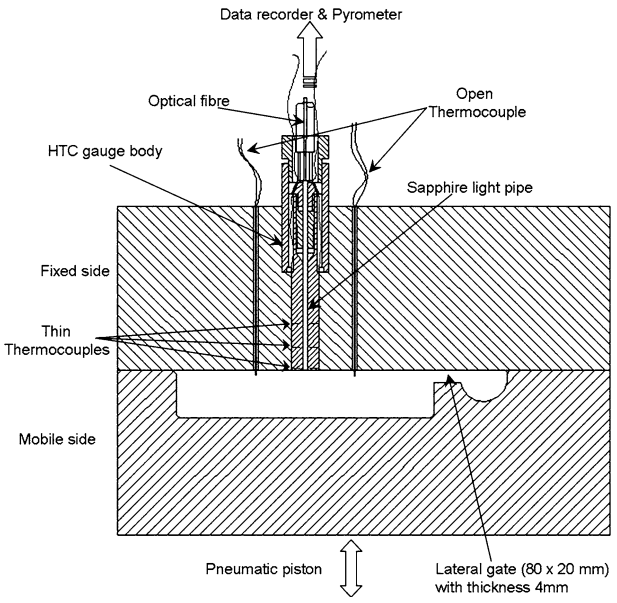

Fig. 1—Top view cross section of the die instrumented with HTCG and open thermocouples and the schemas of the experimental setup.

Table III presents a summary of the experimental conditions.

B. *Temperature Measurement*

The temperature measurements were performed with the HTC gage (HTC gage). It consists of a cylindrical housing fabricated from the same steel as the die that is inserted in the fixed part of the die (HTC gage body in Figure 1). Hence, the surface of the gage is a part of the die surface and is positioned horizontally in the center of the die cavity, as shown in Figure 1. The HTC gage was designed for high-pressure die casting and is described in detail in References 11 and 12. It is now adopted to perform measurements in HPDC, GDC, low pressure, or squeeze casting in industrial conditions without any intrusion into the casting. The HTC gage is able to measure the temperature at the casting surface and the temperature profile in the die using two principles of measurement.

Table I. Chemical Composition of X38CrMoV-5 Steel (Equivalent AISI H11)

Element pct	C	Mn	Si	S	P	Cr	Mo	V	Fe
X38CrMoV-5	0.396	0.36	0.94	< 0.003	0.009	5.05	1.25	0.47	balance

Table II. Chemical Composition of Al-9Si-3Cu and Al-7Si-0.3Mg

Alloys	Cu	Zn	Si	Fe	Ti	Ni	Mn	Mg	Pb	Sn
Al-9Si-3Cu	2.0 to 3.5	1.2	8.0 to 11.0	1.2	0.15	0.3	0.1 to 0.5	0.1 to 0.5	0.5	0.1
Al-7Si-0.3Mg	0.1	0.1	6.5 to 7.5	0.2	0.08 to 0.25	0.1	0.1	0.35	0.05	0.15

Table III. Summary of the Experimental Conditions

Alloys	Solidification Range (°C)	Pouring Temperature (°C)	Initial Die Temperature (°C)	Number of Tests		Measured Coating Thickness Scale (μm)
				TiO_2	Graphite	
Al-9Si-3Cu	590 to 507	750	200 to 210	17	15	5 to 180
Al-7Si-0.3Mg	615 to 554	750	200 to 210	25	18	5 to 150

First, the casting surface temperature is measured by a pyrometer. The infrared radiation emitted from the cast metal is transmitted through the center of the gage by a sapphire crystal light pipe (2-mm diameter) to an optical fiber, which is connected to a pyrometer.

The pyrometer translates this radiation into temperature according to Planck's law of radiation.[13,14] In order to perform this calculation, the emissivity of the casting surface at the pyrometer sensor wavelength is needed. It is determined by a specific method, as described in Section C–2.

Second, temperatures within the die are measured by K-type sheathed thermocouples with external diameter of 0.25 mm. Six thermocouples (type K) are installed at three different positions: 1, 10, and 20 mm below the die surface, as illustrated in Figure 1. They are paired for redundancy. A computer controls the acquisition of data with a system developed for this purpose.

High-pressure die casting uses the deposition of a very fine film of lubricant on the die surface (a few nanometers), in marked contrast to the thick coatings used in permanent mold casting. Therefore, to prevent the thicker coatings affecting pyrometer performance, the surface of the sapphire in the die cavity was protected during the application of the coating.

C. *Calibration of Pyrometer*

1. *Determination of the transmissivity of the pyrometric chain*

In order to ensure the accuracy of the measurement from the HTC gage, the HTC gage connected to the pyrometer was calibrated using a black body. The method simply consists of the measurement of a black body temperature in the range 350 °C to 800 °C by the pyrometric chain (HTCG + optical fiber + pyrometer). Any difference between the pyrometer readings and the black body temperature is caused by the transmissivity of the chain. Therefore, the difference is corrected by changing the transmissivity factor until the pyrometer reading corresponds to the black body temperature.

Initially, there was a difference of about 10 °C between the black body temperature and the temperature indicated by the pyrometer. A much better agreement between them (less than 0.5 °C) was found when the transmissivity of the pyrometric chain (HTCG + optical fiber) was set at 0.3425.

2. *Estimation of the emissivity of the casting surface*

To measure temperature, a pyrometer uses a portion of the energy being emitted by a material surface. Emitted radiation is governed by Planck's law of radiation in which any emitting material has an efficiency characterized by a coefficient called emissivity (ε). The emissivity ε of the part can vary with wavelength and is a critical parameter for accurately determining temperature with a monochromatic pyrometer.[13,15,16] In the case of solidification, determination of ε is not an easy task because the casting surface undergoes a phase change and the alloy surface may also oxidize. These changes influence the value of ε. For this reason, ε must be determined under conditions as close as possible to those of the actual casting processes.

An experimental method illustrated in Figure 1 was set up to determine the emissivity for the alloys. It consists of the same permanent mold that was instrumented with the HTC gage in the center of its cavity. Two K-type thermocouples are inserted into the die at a distance of 15 mm on the left and right of the gage on the same level as the sapphire light pipe. The wires (chromel and alumel) of the thermocouples enter 1 mm into the die cavity. The hot junction is not connected

(open thermocouples), so that the hot junction is created when the melt impinges the wires during die filling. Therefore, the thermocouples and pyrometer readings are triggered simultaneously. During solidification of molten alloys, the temperature readings from the pyrometer and the thermocouples are compared. As the thermocouples and the pyrometer should measure the same surface temperature, the two readings must coincide. The emissivity setting of the pyrometer is modified until there is a good correlation between the two readings. Two pyrometers [IMPAC ISQ (IMPAC France, 6, rue de I'Expansion, F-67150 Erstein, France) and MIKRON M380 (MIKRON® INSTRUMENT, 16 Tornton Road, Okland, New Jersey, 07436,USA)] were used, which were fabricated from different materials and had different spectral sensitivities.

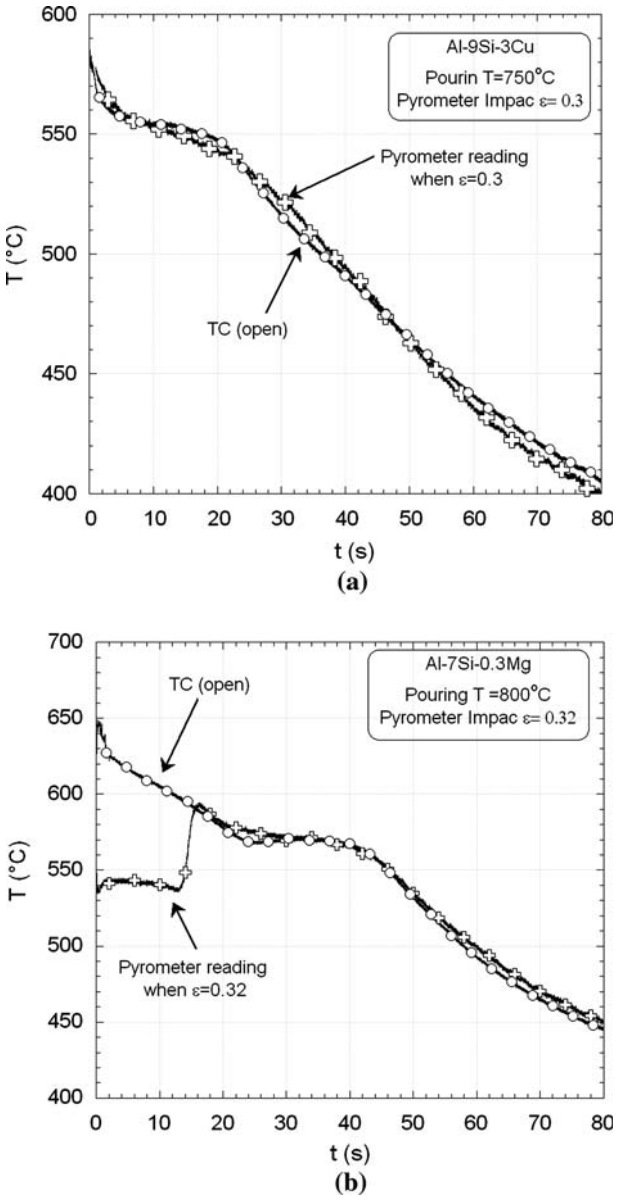

Fig. 2—Thermocouple readings compared to pyrometer reading: (*a*) for Al-9Si-3Cu poured at 750 °C and (*b*) for Al-7Si-0.3Mg poured at 800 °C.

Table IV. Values of Emissivity of Two Alloys Al-9Si-3Cu and Al-7Si-0.3Mg as Determined by Two Pyrometers (IMPAC and MIKRON)

Pyrometer	Spectral Response (μm)	Al-9 Si-3Cu	Al-7 Si-0.3Mg
IMPAC ISQ	0.8 to 1.05	$\varepsilon = 0.3$	$\varepsilon = 0.32$
MIKRON M680	0.65	$\varepsilon = 0.26$	$\varepsilon = 0.2$

As can be seen in Figure 2 (a) (Al-9Si-3Cu), when the emissivity (ε) on the pyrometer was set on 0.3, the two readings were similar. At around 500 °C, there is a disagreement of about 5 °C. This is equivalent to a variation of emissivity of approximately 0.01, which is the smallest increment by which the two equipments can be adjusted. The maximum temperature in that experiment was within the solidification range (*i.e.*, the casting is partially solid at the end of filling). It is possible to obtain temperatures in the die above the liquidus at the end of filling if one increases the pouring temperature of the alloy. In an attempt, the alloy Al-7Si-0.3Mg was superheated to 800 °C. Figure 2(b) compares the two temperatures of the casting surface measured by open thermocouple and by the pyrometer with the emissivity set to 0.32. At the highest temperatures, the two readings do not compare well. However, at lower temperatures, the fit is correct. The transition between the two ranges is sudden at 15 seconds. It is expected that there should indeed be a sudden change of emissivity at the eutectic temperature due to the emissivity of the silicon phase. Nevertheless, the choice of 0.32 for the emissivity allows us to get a reasonable fit from a temperature slightly over than the eutectic (590 °C). In the following experiments, the alloy is superheated at 750 °C, and it is partially solidified when it reaches the cavity. As a result, a good fit is obtained with a constant emissivity of the casting for the two alloys (Al-9Si-3Cu and Al-7Si-0.3Mg) and the two monochromatic pyrometers. Table IV summarizes the results after casting in these conditions.

The determined values of emissivity are in a good agreement with values presented in the literature for the emissivity of aluminum alloys,[16] although such values are invariably subject to uncertainty arising from the effect of the thickness of the surface oxide layer.

III. RESULTS

A. *Raw Data and Inverse Method Results*

1. *Raw data*

Figure 3 shows typical raw data for Al-9Si-3Cu during one cycle. The temperature variations of the alloy surface and at the three positions in the die measured by the HTC gage are plotted as a function of time. The curve marked with the plus symbol shows the surface temperature of the cast alloy. Its maximum value is over 580 °C just after die filling, which corresponds to about 82 pct liquid. The liquid has indeed cooled in the ladle and the sprue to the point of partial solidification.

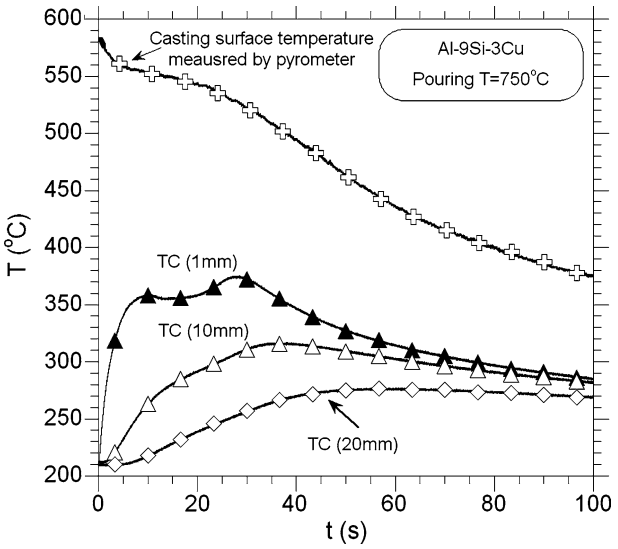

Fig. 3—Raw data collected from the measurements with the HTC gage.

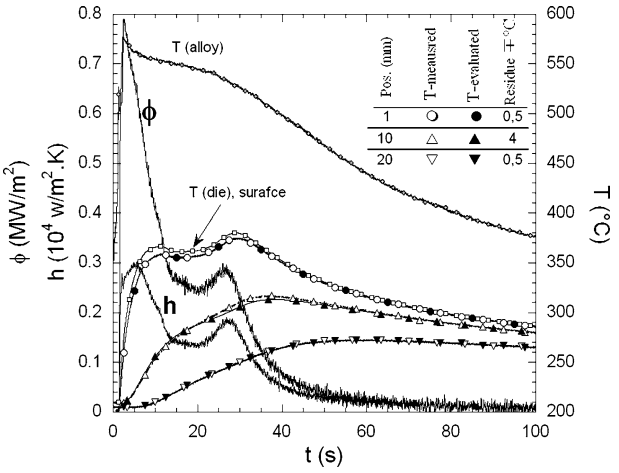

Fig. 4—Heat flux (q), die surface temperature, and HTC as a function of time. Also included are the die temperatures at 1, 10, and 20 mm and recalculated values at the same positions (Al-9Si-3Cu/white coating/pouring temperature is 750 °C).

Just after die filling, the temperature difference (ΔT) is large, which results in a sharp decrease in the temperature of the casting for the first 5 seconds. During this time, the temperature of the die increases and ΔT then becomes smaller. As a consequence, the rate of cooling decreases. Moreover, the casting is close to the eutectic, which is an additional reason for the temperature to show an inflection at that point. The steady fall continues until the temperature reaches 518 °C. Then, the cooling rate increases again and the fall becomes stronger until the end of the cycle. After approximately 35 seconds, the casting temperature has fallen to its solidus temperature (507 °C for Al-9Si-3Cu). This time can be considered as the apparent solidification time of the casting.

The temperatures in the die respond largely as expected, except for the thermocouple just 1 mm under the die surface. Following a rapid rise to 358 °C in the first 10 seconds after filling, the temperature drops by 4 °C, but then begins to rise again at 15 seconds, to a peak of 374 °C after approximately 30 seconds. This two-peaked behavior occurred more or less in all our experiments.

2. *Determination of the HTC and the heat flux at the casting-mold interface*

For each of our tests, the temperature readings at the positions 1, 10, and 20 mm during the cycles have been recorded with a sampling frequency of 200 Hz. The two sets of data at 1 mm and at 20 mm have been analyzed using an inverse method based on Beck's iterative method to evaluate the heat flux density (Wm^{-2}) at the die surface.[17] The detail of this Inverse method (IM) can be found in Reference 18.

From the heat flux density evaluated at the interface, the temperature of the die surface is determined by a direct method using the heat flux density as an input, and the temperature at each position 1, 10, and 20 mm is evaluated as a function of time and compared to the recorded temperatures. The predicted temperature at 10 mm must agree within ± 10 °C over the entire cycle before we accept the IM evaluation.

Figure 4 shows an example of the determination of heat flux density at the casting-mold interface. As can be seen, the heat flux triggers simultaneously with both the die surface temperature and the alloy surface temperature, indicating the arrival of the molten alloy in front of the HTC gage. The heat flux density reaches a maximum value over 700 kW/m^2, and then undergoes a sharp fall to about 250 kW/m^2 during the next 10 seconds. Then, it rises again to about 320 kW/m^2 before the occurrence of the final fall and the end of the cycle.

The heat flux density at the interface as a function of time enables the evaluation of the mold surface temperature by a direct resolution of the heat conduction problem. The result is shown in the curve marked with open squares in Figure 4. The surface temperature follows a very similar trend to the temperature at 1 mm, with a maximum difference between them of about 10 °C, which is consistent with the heat flux measured. When the die surface temperature starts to decrease, this difference reduces toward zero, showing the reduction of the thermal gradient through the die when the molten metal becomes solid.

Also included in Figure 4 are measured and recalculated die temperatures. The disagreement between the evaluated and measured temperature does not exceed 7 °C. The good fit implies that the critical distance of the first thermocouple from the surface is correct. Following verification of the temperature data produced from the IM, the evolution of the HTC was determined as a function of time by Eq. [1]

$$h(t) = \frac{q(t)}{T_{sc} - T_{sd}} \qquad [1]$$

where h, q, t, T_{sc}, and T_{sd} are, respectively, the HTC, heat flux density evaluated by the inverse method, the

time, the casting surface temperature measured by the pyrometer, and the die surface temperature derived during the evaluation of q.

The evaluated HTC at the casting-mold interface as a function of time is also shown in Figure 4. The shape of the evolution of HTC is similar to that of heat flux. The maximum value is over 2.8 kWm^{-2} K^{-1} and then it decreases to 1 kWm^{-2} K^{-1} during the first fall. Twenty seconds later a second peak is observed to reach about 1.8 kWm^{-2} K^{-1}. After the second peak, the final fall occurs toward zero, probably due to the formation of an air gap at the casting-mold interface. It is important to notice that this study has involved a large number of casting cycles. The shape and the time variation of HTC are consistent from cycle to cycle. This reproducibility allows us to observe variations in response to changes in die coating material and thickness, and for different alloys.

3. *Error analysis*

The intrinsic time response for 0.25-mm ungrounded thermocouples is around 10 ms.[19,20] This time response is around 1.5 pct of the time duration of the heat input (the time during which heat flux density reaches its maximum value from zero) in our calculation. Therefore, it should not have any significant effect on the maximum value of evaluated heat flux. Nor, therefore, should it affect the HTC at the casting-mold interface.[12] However, there are a number of other sources of inaccuracy in the determination of the HTC at the casting-mold interface. They are related back to the inaccuracies in the following: (1) temperature measurements, (2) the thermal properties of the mold, and (3) the uncertainty in the location of the first thermocouple (1 mm from the mold surface). Following the analysis of Dour *et al.*,[12] the error in the heat flux density can be determined from the following equation:

$$\frac{dq}{q} = \frac{dT}{T} + \frac{d\lambda}{\lambda} + \frac{1}{2}\frac{da}{a} + \frac{q_{\max}}{\lambda\ T}\ dz \qquad [2]$$

where

T = the temperature of the die at any time. Its value is between 200 °C and 400 °C in our experimental trials. According to the IEC 584 norm, the tolerance of class 1 K-type thermocouples is ± 1.5 °C over the entire range of temperature measurements, and the proposed error due to the fitting of the thermocouple in the gage is 10 °C.

λ = the thermal conductivity of the die taken to be constant at 29 Wm^{-1} K^{-1} in the present inverse method calculations. According to the measurements reported in Reference 21, an uncertainty of ~1.5 Wm^{-1} K^{-1} should be noted.

a = the thermal diffusivity of the die taken to be constant at $6.9{\cdot}10^{-6}$ m^2 s^{-1} in the present inverse method calculations. According to the measurements performed in Reference 21, an error of order $0.1{\cdot}10^{-6}$ m^2 s^{-1} should be noted.

$q_{\max}$ = the peak value of the evaluated heat flux density (around 0.8 $MW{\cdot}m^{-2}$).

dz = the inaccuracy in location of the thermocouple. Based on the precision of the hole drilling operation given by the manufacturer, its tolerance is ± 0.03 mm.

With the previous values and precisions of mentioned parameters, the error on heat flux density was found to be around 9 pct.

From Eq. [1], the deterministic uncertainty in HTC at the casting-die interface can be determined by Eq. [3]:

$$\frac{dh}{h} = \frac{dq}{q} + \frac{dT_{sd}}{\Delta T} + \frac{dT_{sc}}{\Delta T} \qquad [3]$$

where $dT_{sd} = dq/qT_{sd}$ according to Reference 12, and ΔT is the value of the temperature gap at the interface at a given instant.

In addition to the 5 °C error in casting surface measurement due to the emissivity as discussed in Section II–C–2, the errors in temperature measurements introduced as a result of eventual heat losses between the sapphire light pipe and the surrounding housing was investigated using two-dimensional simulation.[22] The error in casting temperature measurements was then found to be less than 15 °C.

Incorporating all of these inaccuracies, Eq. [3] yields an error of around 30 pct in the peak of the HTC. Furthermore, this error is drastically dependant on the temperature jump at the interface and, hence, it changes with time. As illustrated in Figure 5, the error curve is low at the peak of h (~30 pct) when ΔT is high and increases with the reduction of ΔT. It is of course very large when ΔT is difficult to determine.

The time dependence of the error in evaluating HTC at the casting-mold interface has been reported in Reference 23. In spite of different experimental and analytical methods that have been used in Reference 23, the error in HTC and its increase with time are fairly comparable to those presented in Figure 5.

4. *Interpretation*

One of the interesting phenomena associated with the temperature variation at the interface is that the initial fall of the die surface temperature is not monotonic. It is followed by a second increase at 15 seconds. This

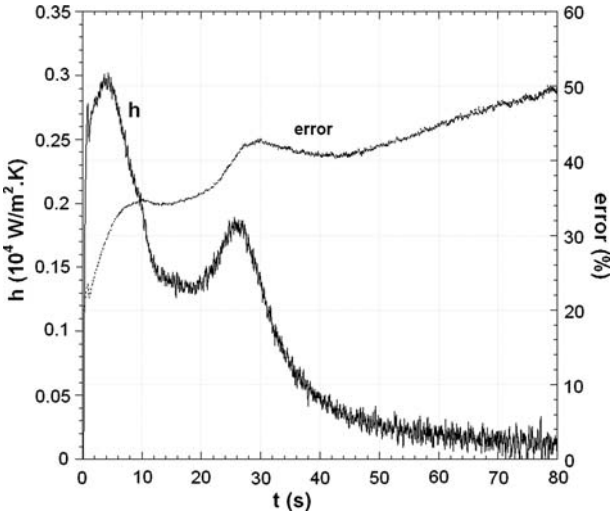

Fig. 5—Relative error in evaluated HTC at the casting-mold interface.

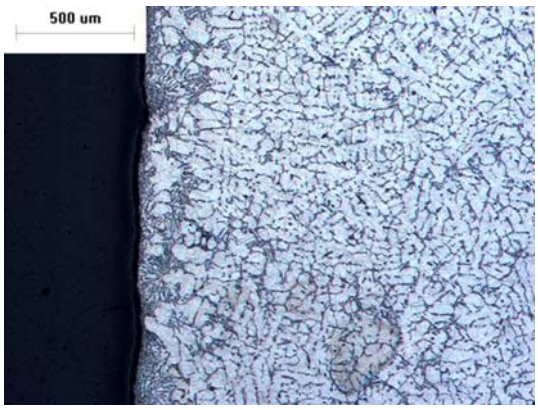

Fig. 6—Optical micrograph from a section of the casting (Al-7Si-0.3Mg) taken from the area of contact with the HTC gage.

phenomenon has been observed for both alloys used and it seems to occur independently of coatings. This phenomenon can be related to the second peak in the heat flux (q) and HTC curves, as can be seen in Figures 4 and 5.

Several castings were sectioned and examined metallographically to try to identify the cause of this second peak. A typical micrograph is shown in Figure 6, where the distinctive features of eutectic liquid exudation are evident. A plausible sequence of events that could explain the second peak is as follows. Close examination of Figure 4 suggests that the curves of heat flux and HTC stop dropping sharply a few seconds after the alloy temperature falls to the eutectic temperature (end of the dendritic solidification interval). It seems that the curves of heat flux and HTC drop with the solid fraction. Moreover, second peaks occur when the solid fraction is around 85 pct and the casting shell might be gaining some measure of rigidity. As it begins to thermally shrink, there are enough liquid feed channels remaining open to permit the residual enriched liquid to be forced through under metallostatic pressure into the small gap. The fresh contact of liquid with the die coating decreases thermal resistance, leading to increased HTC, and hence increased heat flux and surface die temperature. The slow buildup to the second peak implies that the exudation is itself slow, or else it occurs over time in numerous places on a very small scale.

After the HTC reaches this second peak, we observe that the casting surface is almost solidified, with the remaining liquid likely to be in isolated pools. Therefore, an air gap due to the contraction of the aluminum alloy by solidification should start to form at the interface. This air gap separates the casting surface from the die. The low conductivity of air causes a dramatic increase in the thermal contact resistance at the interface. That is why a significant continued fall of HTC is observed after the second peak, and it continues until the end of solidification when the HTC falls to an undetectable value. This result shows that the variation of HTC with time during solidification is not uniquely due to the formation of an air gap, as suggested by some investigators (*e.g.*, Reference 24), but also to the variation in the contact conditions between the casting and the mold surface during the development of solid fraction from the very beginning of solidification.

Moreover, the phenomenon of the two peaks is commonly observed in the heat flux (or mold heating rate) curves and occasionally in the HTC curves for the permanent mold casting of hypoeutectic alloys.[5,10,18,25–30] Wei *et al.*[29] concluded on the basis of heating rate peaks that this was a result of the nonmonotonic evolution of the latent heat of fusion during solidification. The Al-Si alloys have a high rate of latent heat release (per unit temperature) when the primary dendrites first form, and an even higher rate when the eutectic starts to solidify. This does correspond well to heat flux peak positions, but the explanation cannot account for a second peak in HTC, which is determined by interface properties, not the latent heat of the surrounding material. A change only in latent heat release rate, without a change in the nature of the interface, would be expected to show a peak in heat flux, but a steady decrease, or at best a plateau, in HTC.

Schmidt and Svensson[10] (supplement III) describe this later stage in the evolution of HTC during solidification as the semisolid stage in HTC evolution. However, no reason for this second increase in HTC(t) was proposed. Hwang *et al.*[30] also observed double peaks in HTC, even more pronounced than the results presented here, and postulated that it was caused by the eutectic liquid penetrating the partially solid framework and flowing into the gap. Kim and Lee[27] observed another anomalous trend in HTC, but only on the inside of a ring mold. They explained it as a form of "burst feeding," but it is not clear if a similar explanation would apply in the current experiments. They also observed a slight second peak in HTC on the outer surface, but only for one alloy and only for the "white" diecoat.

The microstructure in Figure 6 clearly supports the hypothesis proposed by Hwang *et al.*[30] that exudation of the eutectic liquid is responsible for a change in the gap dimensions at the later stages of solidification at the surface. There are two possible situations with exudation: (a) the liquid could find a preferential path through the shell and then spread sideways through the existing gap; or (b) it could seep evenly through the interdendritic spaces. Based on our observations, we could not make a determination between these possibilities, but the first option could certainly lead to significant scatter in the magnitude of the second peak. The surface tension effects between the melt and die coat would also be an important factor in either case.

B. *Effect of Coating Thickness and Composition*

1. *Maximum values of alloy and die surface temperatures*

Figure 7 shows the variation of the maximum temperature of both the alloy surface and the die surface as a function of the coating thickness during several cycles of permanent mold casting. The curves marked with white triangles represent the cycles performed with the white coating, and these curves marked with black

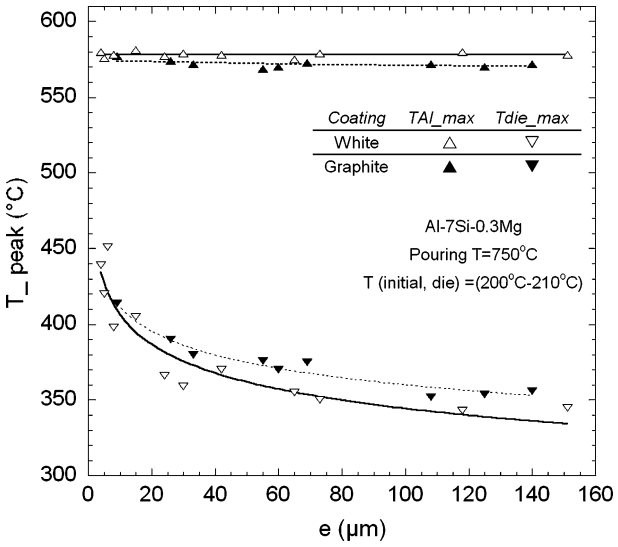

Fig. 7—The variation of die and alloy surface temperature as a function of coating thickness (e) for two kinds of coating (white and graphite) during casting cycles of alloy Al-7Si-0.3Mg.

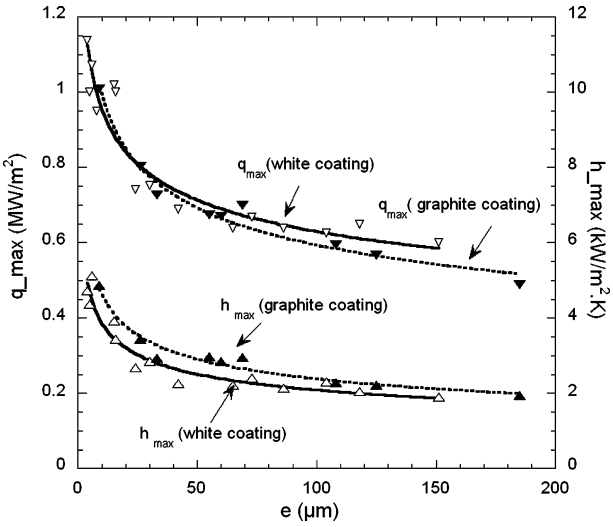

Fig. 8—Maximum of heat flux and HTC as a function of coating thickness for a series of casting of the Al-7Si-0.3Mg alloy with both white and graphite coatings.

triangles represent the cycles performed with the graphite coating.

In general, for the two coatings, the peak values in the alloy's surface temperature do not vary with the coating thickness and remain fairly constant. However, the magnitude of the peaks in the die surface temperature decrease as the coating thickness increases, but the variation is not linear and is much more noticeable for coating thicknesses of less than 20 μm.

Furthermore, the peaks in die and alloy surface temperatures seem to be fairly similar for the two coatings at thicknesses less than 20 μm. The slight difference observed in the peak values of the die and casting temperature for the two coatings is consistent with the fact that ceramic coatings are better insulators than graphite coatings.

2. *The maximum of the heat flux and the HTC*

Figure 8 shows the peak values of the HTC and heat flux as a function of coating thickness for some casting cycles separately performed on the die with white and graphite coatings. The alloy used was Al-7Si-0.3Mg. The curves marked with black triangles represent the casting cycles produced with graphite coatings, and those marked with white triangles represent the castings produced using a white TiO_2 coating.

Generally, for the two coatings, the peak values of both q and HTC decrease while the coating thickness increases. For example, for the cycles performed with the white coating, q decreases from 1.15 MWm^{-2} to about 0.65 MWm^{-2} and the HTC decreases from about 4 $kWm^{-2}\,K^{-1}$ to 2.4 $kWm^{-2}\,K^{-1}$, while the coating thickness changes from 5 μm to 120 μm.

Meanwhile, the variation of peak values of q and HTC as a function of coating thickness is fairly similar for both coatings. The peak values of q and HTC are comparable for both coatings.

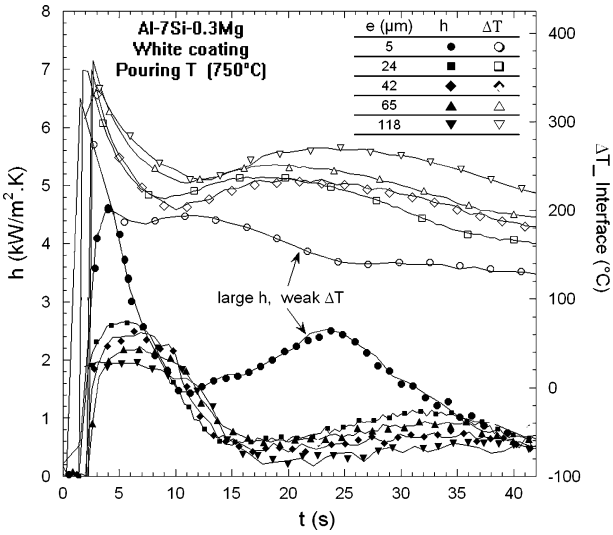

Fig. 9—The variation of the temperature jump and the HTC at the casting-mold interface as a function of cycle time (white coating).

3. *Variation of the HTC and the temperature jump at the interface while varying coating thickness*

Figure 9 shows the variation of both HTC and ΔT at the casting-mold interface, as a function of time for different castings produced using different thicknesses of coating.

Generally, $\Delta T(t)$ decreases dramatically after the die is filled and continues to decrease for around 10 seconds, at which time it begins to increase steadily. Then, it decreases until the end of solidification, but remains around 100 °C for an extended period. The thinner coating produces a small thermal contact resistance and hence the best HTC, which causes a rapid increase in the die surface temperature and hence a lower $\Delta T(t)$ during solidification.

On the other hand, for a range of coating thicknesses from 24 to 118 μm, the HTC shows a steady second rise after about 20 seconds of solidification. However, the second rise of HTC for the smallest thickness (5 μm) starts at about 10 seconds to reach a second peak of 2.5 kWm^{-2} K^{-1}. Generally, after around 40 seconds, it appears that there is no detectable effect of coating thickness on the HTC. This is probably caused by the creation of an air gap between the casting and the die, with such a low thermal resistance that it dominates the HTC.

4. *Variation of the HTC as a function of time for different coating compositions*

The effect of coating composition on the HTC was investigated by plotting the variation of HTC as a function of time for two castings produced with two different thicknesses (thin and thick) of white coating. These are juxtaposed to the variation of HTC for another two castings produced with graphite coating of comparable thicknesses (Figure 10). The initial peaks are a very similar shape and have amplitudes that seem to depend only on coating thickness, with the peak value increasing with decreasing thickness, as would be expected. However, the second peaks reverse this trend and show a strong dependence on coating material and only a weak dependence on coating thickness. A graphite coating produces not only a much higher second peak, but also a shortened time to reach that peak.

5. *Interpretation*

As we mentioned in Section III-B-2, the HTC and the heat flux at the casting-mold interface decrease as the coating layers become thicker. This finding is simply due to the increase in resistance to the heat flux that occurs as a result of the increase in coating thickness. The HTC and the heat flux are apparently more sensitive to coating thicknesses at the thinner layers.

Generally, die coating consists of a fine powder, held together by a binder (usually sodium silicate). When the coating is sprayed onto the preheated die surface (about 200 °C), the remaining water vaporizes and generates pores filled by air that are found in the coating structure (Figure 11). This means that there is imperfect contact between the coating layer and the die and between the coated die and the casting, as illustrated in Figure 12. So, not only is there thermal resistance due to the coating layer itself, but in addition, the application of the coating generates additional thermal resistance to the heat flux because of the imperfect contact between casting-coating and perhaps coating-die interfaces known as constriction thermal resistances. That is why the application of even a thin layer of coating causes a significant fall in HTC at the interface. With thinner layers, the condition of the casting-coating and perhaps coating-die contact should have the dominant effect on the HTC. As the layer thickness increases, the contribution of coating composition increases in significance. That is the reason for the small difference in the peak values of HTC for both coatings when the coating thickness is over 100 μm, as can be seen from Figures 8 and 10. However, this difference is small, even if the graphite has a much better intrinsic thermal conductivity than the TiO_2 white coating. In fact, the apparent

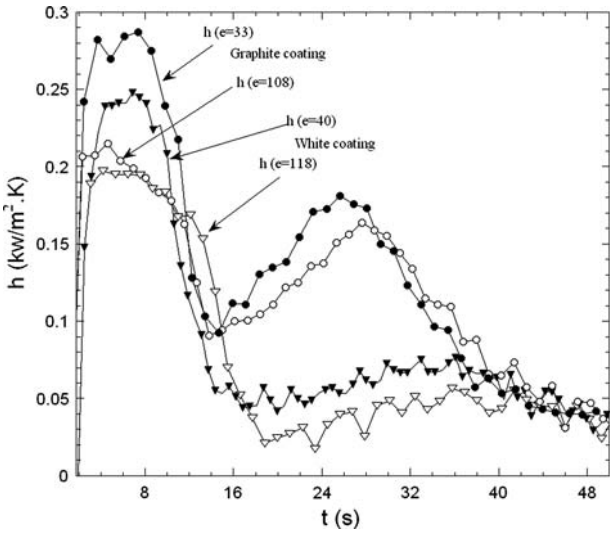

Fig. 10—The effect of coating type on the evolution of HTC of Al-7Si-0.3Mg alloy. Open symbols are the thin coating and solid symbols are the thick coating.

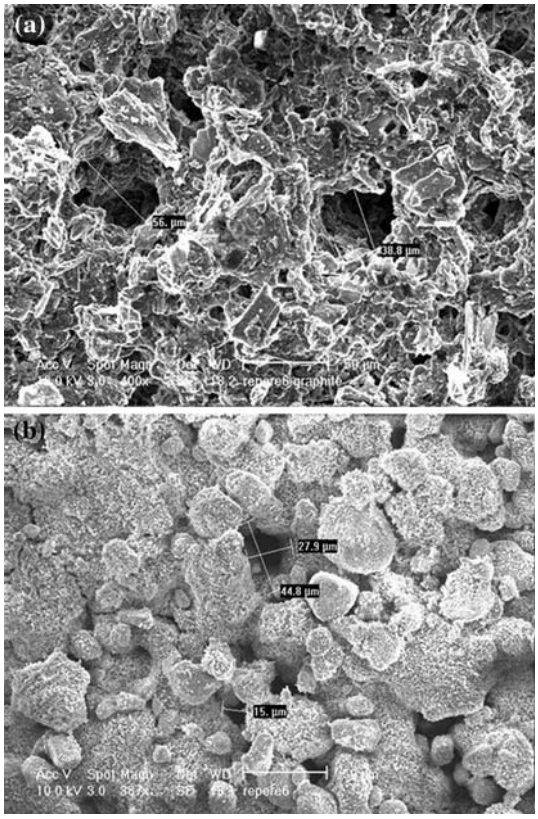

Fig. 11—E-SEM micrograph showing the porous microstructure of the coating applied to the die surface ((*a*) graphite and (*b*) TiO_2 white coatings). The magnification bar corresponds to 50 μm.

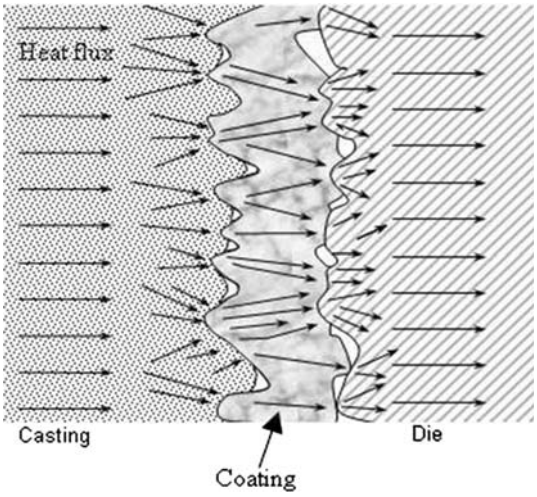

Fig. 12—Three components of the casting-mold interface (casting-coating, coating, and coating-die interfaces) in permanent mold casting and the heat flux density while crossing this interface.

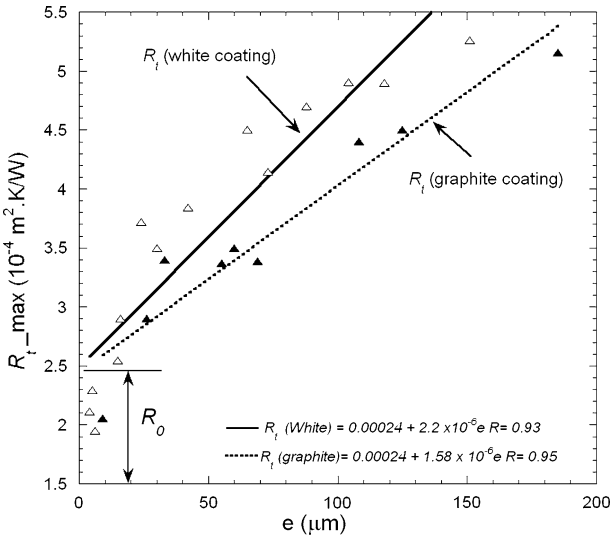

Fig. 13—R_t at the casting-mold interface using Al-7Si-0.3Mg alloy as a function of two kinds of coating thickness (graphite and white coatings) (pouring temperature is 750 °C and initial die temperature is 200 °C to 210 °C).

thermal conductivity of these coatings should not be so different because the coating film has a porous structure. The large quantity of air in the coating structure means that the thermal conductivity of the applied coating is dominated by the thermal conductivity of the air pockets.

On the other end, the nature of the coating seems to have a large influence on the second peaks. The use of graphite coating leads to a more pronounced peak, whatever its thickness (Figure 10). It is only for extremely thin thicknesses of white coating that a second peak can be seen (Figure 9). Some more work is currently being carried out to fully interpret this phenomenon.

IV. MODELING OF THE HTC PEAK AND VARIOUS EFFECTS

A. *Modeling of HTC Peak*

The mathematical modeling of HTC at the casting-mold interface has undergone rapid development within the last decade, because casting simulation software needs accurate HTC parameters in order to yield reasonable results. We will not present a new model in this article, but our experimental results should help clarify and analyze the basic elements that are usually used to model the HTC in permanent mold casting. Such analysis is useful for anybody aiming at a rigorous model that takes into account the casting conditions.

By definition, the HTC at the casting-mold interface is the inverse of the thermal contact resistance (R_t = 1/HTC). If we transform the peak values of HTC, which are presented in Figure 8 to R_t, we obtain the R_t as a function of coating thickness, as illustrated in Figure 13. For the range of coating thicknesses between 0 and 200 μm, the minimum of the R_t shows a continuous increase for both coating type while coating thickness increases. As can be seen, it is possible to linearize the relationship between R_t and coating thickness (e) with a good correlation coefficient (0.93 and 0.95).

In general, R_t at the casting-mold interface is the sum of a series of resistances across the interface.[10,19,28] These resistances are the resistance due to the contact roughness (R_o) (constriction resistance), the resistance due to the coating (R_c), the resistance due to the formation of the air gap (R_a), and the resistance due to radiation (R_r). With the exception of R_r, which is known to be connected in parallel, all other mentioned resistances are considered to be connected in series. The contribution of the resistance due to radiation is negligible in aluminum permanent mold casting, because the temperature of the casting is relatively low and the emissivity is low.[31] Then, R_t can be expressed by Eq. [4].

$$R_t = R_o + R_c + R_a \quad [4]$$

It is clearly observed in Figures 8 through 10 that the largest heat extraction occurs at the beginning of solidification when the alloy is still mostly liquid, because the contact between the casting and the coated die is good and the die surface is colder. This phase of solidification is of the greatest interest, because the microstructure of the casting is largely determined before the creation of the air gap. At that stage, R_a is negligible and will be ignored in the following analysis. Then, if we assume the coating properties are independent of applied thickness, Eq. [4] becomes

$$R_t = R_o + \frac{1}{\lambda_c} e_c \quad [5]$$

where λ_c is the thermal conductivity of the coating, e_c is the thickness of the coating, and R_o is the intercept value at $e_c = 0$, which from Figure 13 is equal to about 0.25×10^{-3} m^2 kW^{-1}. The range of R_o depends on the

conditions of contact at the casting-coating and coating-die interfaces. The term R_o is still a problem for modeling R_t, because (1) the relative contribution of these two interfaces (casting-coating or coating-die) is not well understood, (2) it is also not yet clear which parameter of surface roughness is predominant on this resistance, and (3) the role of surface tension of the casting liquid is not well understood.

The slopes of the fitted straight line in Figure 13 represent the inverse of the apparent thermal conductivities of the coatings. According to our result, the thermal conductivities of the white and the graphite coatings are determined to be 0.45 $Wm^{-1} K^{-1}$ and 0.6 $Wm^{-1} K^{-1}$, respectively. These values are in good agreement with the values obtained in the literature for these kinds of coatings. Cheisa, Hallam *et al.*, Schmidt, and Kim and Lee[4,8,10,27] measured the thermal conductivity of various white coatings to be 0.25 $Wm^{-1} K^{-1}$, (0.2 to 0.4) $Wm^{-1} K^{-1}$, (0.6 to 0.8) $Wm^{-1} K^{-1}$, and (0.12 to 0.42) $Wm^{-1} K^{-1}$, respectively. These values of the thermal conductivity of the white coating are consistent with our results, considering that the coatings are heterogeneous in nature and properties can vary with material supplier's formulations and the application techniques.

B. *Effect of Air Gap*

From Figures 9 and 10, we observe that after about 40 seconds of solidification, the influence of coating thickness and composition on HTC disappears. It appears that the reason for this is linked to the formation of an air gap at the casting-mold interface when solidification is complete. Because the heat conductivity of air is small (0.05 $Wm^{-1} K^{-1}$ at 400 °C), this gap offers a resistance to heat transfer that is larger than that of the coating. As a result, heat transfer is governed by the resistance of the air gap (R_a) and the two others resistances (the resistance due to the imperfection of contact (R_0) and that of the coating (R_c) become negligible).

In fact, when R_a becomes predominant, Eq. [5] becomes

$$R_t \approx \frac{e_a}{\lambda_a} \qquad [6]$$

The critical air gap thickness found by this relation when R_a becomes predominant is given by

$$e_a \geq \left(R_o + \frac{e_c}{\lambda_c}\right)\lambda_a \qquad [7]$$

where e_a is the air gap thickness and λ_a is the air thermal conductivity.

From Eq. [7], one can estimate that the air gap thickness is around 25 μm when it begins to dominate heat transfer process with 100 μm of coating. This is consistent with the measurements of Decultieux[32] and Schmidt[10] that found good correlation between air gap thickness and heat transfer beyond 50 μm.

C. *Effect of Alloy Composition on HTC and Heat Flux Peaks*

Figure 14 (a) shows the variation of the maximum of both the HTC and heat flux density at the casting-mold interface for the two alloys (Al-7Si-0.3Mg and Al-9Si-3Cu) as a function of coating thickness. This series of castings was produced using the die prepared with the white TiO_2-based coating, and all other process parameters remained constant.

When the coating thickness is small (0 to 20 μm), no significant difference is observed in the maximum of both heat flux and HTC for the two alloys. However, when the coating is thicker than 20 μm, the maximum

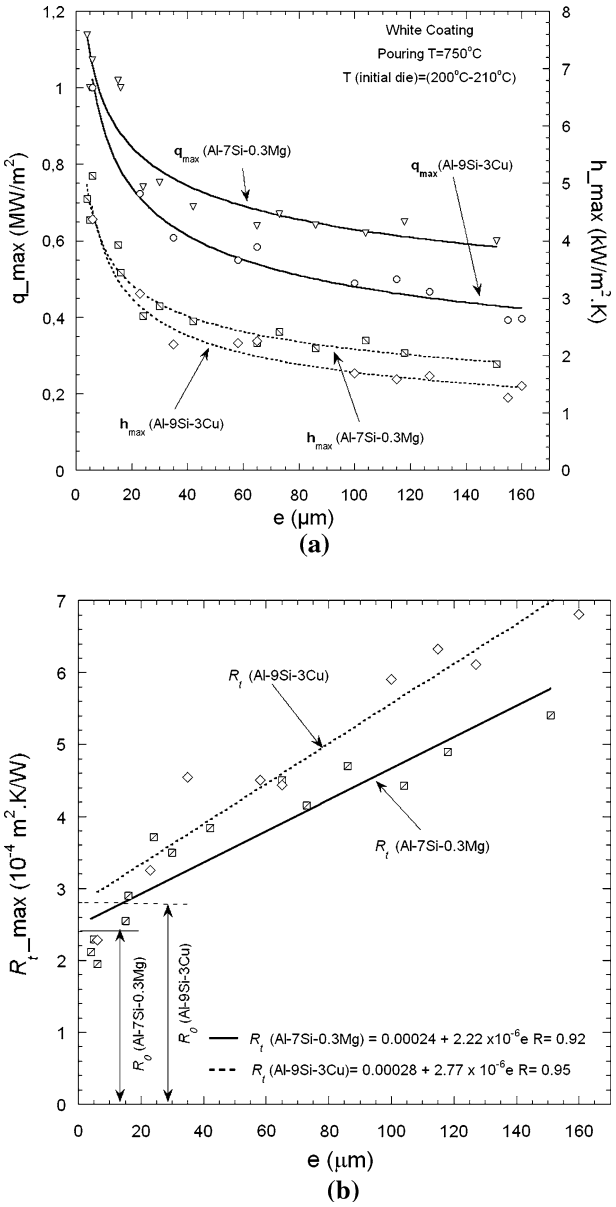

Fig. 14—(*a*) Maximum of heat flux and HTC and (*b*) maximum of R_t as a function of coating thickness for a series of cycles with the Al-9Si-3Cu and Al-7Si-0.3Mg alloys.

values of heat flux for the Al-7Si-0.3Mg alloy become larger than for the Al-9Si-3Cu alloy, whereas only a slight increase in HTC is observed. Such variation in heat transfer with different alloys had been reported in the literature. Bamberger[25] reports that the HTC for the alloy with a small percentage of silicon is larger than that for an alloy with a larger level of silicon. For Schmidt,[10] the alloy composition had no influence on the HTC above the liquidus temperature (in our experiments, the alloy is slightly under the liquidus temperature when the molten alloy arrives at the HTC gage position in the die cavity). Prates[33] showed that HTC increases when the percentage of copper is increased in the alloy composition. The sensitivity of heat flux to the composition could be due, at least in part, to the variation in fraction solid with temperature. The peak heat flux occurs near the liquidus, and the more dilute Al-7Si-0.3Mg alloy has a higher fraction of solid formed (and hence a higher amount of latent heat evolved) within a few degrees of the liquidus. While latent heat evolution can affect heat flux, it does not determine HTC, so an explanation is required for how the composition can influence the nature of the coating-casting interface.

In order to further clarify the effect of alloy composition, we plotted the minima of R_t for both alloys as a function of coating thickness in Figure 14(b) and performed a linear regression. As expected, the slopes of both lines are similar because the same coating was used for these castings. However, R_0 of the Al-7Si-0.3Mg alloy is smaller than that of Al-9Si-3Cu alloy by about 4×10^{-5} m^2 kW^{-1}. The term R_0 is the sum of constriction resistances of the casting-coating interface and the coating-mold interface. The value at the coating-mold interface cannot depend on alloy composition, so the variation in R_0 with alloy must be related to the casting-coating interface. One of the alloy properties that could influence the condition of contact at the interface is the surface tension of the casting liquid. Changing the proportion of the component such as Si and Cu in an alloy composition should influence the surface tension as well as the wetting angle of the liquid casting. Hence, the contact condition between liquid metal and mold should be modified. Recently, Bainbridge[34] reported that the surface tension of the binary alloy is influenced by the composition of the alloy. The surface tension of the Al-Si alloy tends to decrease with increasing amounts of silicon. However, increasing the amount of magnesium above 0.5 pct in the Al-Mg alloys leads to an increase of the surface tension. He also found that varying the amount of copper from 0.5 to 2.5 pct does not have a significant effect on surface tension in the Al-Cu alloy. Based on these results, we estimate that the wetting angle of the Al-7Si-0.3Mg alloy should be smaller than that of the Al-9Si-3Cu alloy. The smaller wetting angles allow the liquid to penetrate deeper into the asperities of the rough coated mold surface. This could be a reason for the smaller R_0 observed in Figure 14(b).

D. *Effect of Coating and Alloy on the Solidification Time*

The solidification time is known to have a significant influence on microstructure and porosity of aluminum castings, and hence, it can influence their structural integrity. It is therefore important to understand the way coating thickness influences the solidification time for aluminum alloys.

From curves such as those shown in Figure 3, the apparent solidification time at the surface of the casting was evaluated as the time from liquidus temperature (615 °C for Al-7Si-0.3Mg and 590 °C for Al-9Si-3Cu) to the eutectic (555 °C for Al-7Si-0.3Mg and 507 °C for Al-9Si-3Cu). The results are summarized in Figure 15. The solidification time for the two alloys increases as the coating thickness increases. The solidification rate appears to be more sensitive to the thinner layers (similarly for HTC) for the reason mentioned in Section III–B–5.

The solidification time of the Al-9Si-3Cu alloy is larger than that of Al-7Si-0.3Mg, because the temperature interval between the liquid phase and solid phase is larger for the Al-9Si-3Cu alloy (about 80 °C) than for the Al-7Si-0.3Mg alloy (about 60 °C). Furthermore, the extra amount of Si increases the latent heat of fusion, by approximately 4 pct in Al-9Si-3Cu. Moreover, the two alloys are poured at the same melt temperature (750 °C). This means that there is about 115 °C of super heat for the Al-7Si-0.3Mg alloy and 160 °C for the Al-9Si-3Cu alloy.

The weak influence of coating composition on HTC leads to a similar small influence on the apparent solidification time. The coating composition has no detectable influence on the solidification time for thinner coatings and at the thicker layers, particularly above

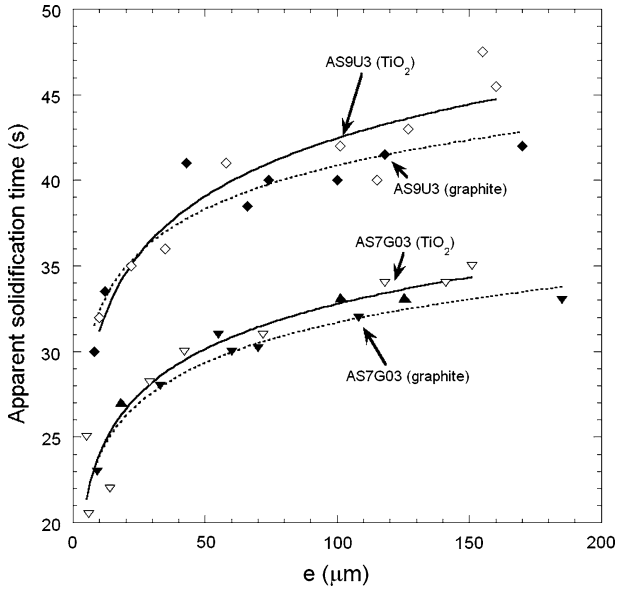

Fig. 15—Apparent solidification time of the Al-9Si-3Cu alloy and the Al-7Si-0.3Mg alloy as a function of coating thickness (white and graphite coatings).

100 μm, the TiO_2-based white coating seems to extend solidification time by up to 4 to 5 pct.

V. CONCLUSIONS

An experimental thermal analysis method suitable for permanent mold casting has been developed. The temperature measurements were performed by a HTC sensor, which measures the casting surface temperature by a pyrometric chain and the temperature throughout the mold wall at three positions (1, 10, and 20 mm) from the mold surface by K-type thermocouples.

The HTC was evaluated at the casting-mold interface in permanent mold casting for two aluminum alloys (Al-9Si-3Cu and Al-7Si-0.3Mg) and two mold coatings (graphite and TiO_2).

The heat flux density and HTC showed two peaks during solidification: one peak occurred in the first few seconds of casting, when the casting was fully liquid or at a low fraction solid. A second, smaller peak occurred during or after Al-Si eutectic solidification at the surface. The magnitude of the major peak depended mainly on coating thickness and not coating composition. In contrast, the minor peak showed a much stronger dependence on coating composition than thickness.

The secondary peak was attributed to the exudation of liquid of approximately eutectic composition, which made fresh liquid contact with the mold coating.

The peak HTC was found to decrease as the coating thickness increased, losing about 50 pct of its value when the coating thickness increased from 10 to 100 μm. The HTC is particularly sensitive to coating thickness for thin coating layers (< 20 μm), although this sensitivity weakens gradually with increased coating thickness.

The peak values of HTC are slightly larger where graphite coatings are used compared to those when TiO_2-based white coating is used. However, this difference is weak compared to the considerable difference in intrinsic thermal conductivity for both coatings. It seems that the coating thermal resistance in permanent mold casting is more dominated by coating porosity than composition.

From the experimental results, the usual model of series resistances applies well. The apparent thermal conductivity of TiO_2 white coating and graphite coating was evaluated to be 0.45 Wm^{-1} K^{-1} and 0.6 Wm^{-1} K^{-1}, respectively. The contact resistance was found to be nearly the same (for the Al-7Si-0.3Mg alloy) and close to 0.25×10^{-3} m^2KW^{-1}. The mechanism for this is currently unclear and will be addressed in future research.

The peaks of HTC and the heat flux are slightly larger during the solidification of the Al-7Si-0.3Mg alloy than the Al-9Si-3Cu alloy. However, their variations as a function of coating thickness are comparable.

The apparent solidification time of Ai-9Si-3Cu was larger than that of Al-7Si-0.3Mg by about 40 pct. It was increased by a rate of 0.06 s/μm as the coating thickness increased, and both are influenced by coating in a similar way as the HTC.

ACKNOWLEDGMENTS

The authors thank the CROMeP Centre in Ecole des Mines d'Albi Carmaux and the director Mr. Bernhart who allowed this work in his research centre. We also thank Mr. Tovar for his contribution during the trials. The authors acknowledge the CROUS for supplying a scholarship to one of the authors (AH), and CAST for actively supporting this activity through a cotutelle agreement with the Université Paul Sabatier and The University of Queensland

REFERENCES

1. F. Chiesa: *AFS Trans*., 1998, vol. 106, pp. 589–94.
2. C. Wu, V. Sahajwalla, and R.D. Pehlke: *AFS Trans*., 1998, vol. 105, pp. 739–44.
3. D. Tomasevic: *Fonderie-Fondeur d'aujourd'hui*, 2004, vol. 236, pp. 20–32 (in French and English).
4. F. Chiesa: *AFS Trans*., 1990, vol. 98, pp. 193–200.
5. G. Sciama, J.-F. Ribou, and CTIF: *Fonderie-Fondeur d'aujourd'hui*, 1997, vol. 169, pp. 23–62 (in French).
6. D. Tomasevic, Y. Longa, and A. Silva: *Fonderie-Fondeur d'aujourd'hui*, 2005, vol. 245, pp. 21–30 (in French and English).
7. V. Davies: *Br. Foundryman*, 1980, vol. 73, pp. 331–34.
8. C.P. Hallam and W.D. Griffiths: *Metall. Mater. Trans. B*, 2004, vol. 35B, pp. 721–33.
9. M.Z. Jahedi and M. Giannos: *Mater. Australia*, 2000, vol. 33, pp. 20–22.
10. P. Schmidt: Ph.D. Thesis, Royal Institute of Technology, Stockholm, 1994.
11. G. Dour, M. Dargusch, C. Davidson, and A. Nef: *J. Mater. Process. Technol*., 2005, vol. 169, pp. 223–33.
12. G. Dour, M. Dargusch, and C. Davidson: *Int. J. Heat Mass Transfer*, 2006, vol. 49, pp. 1773–89.
13. PP. Hervé: *Technique de l'ingénieur*, 1989, Doc R 2735 (in French).
14. PP. Hervé: *Technique de l'ingénieur*, 1989, Doc. R 2737 (in French).
15. *Infrared Thermometers*, User's Manual, Mikron Instrument Company, New Jersey, 1998, p. 23.
16. Impac Electronic GmbH (collective work): *The Pyrometer Handbook*, Frankfurt, 1999, pp. 16–27.
17. Y.-H. Chen and Y.-T. Im: *Int. J. Mach. Tools Manuf*., 1990, vol. 30, pp. 175–89.
18. S. Broucaret, A. Michrafy, and G. Dour: *J. Mater. Process. Technol*., 2001, vol. 110, pp. 211–17.
19. *The Temperature Handbook*, Omega, Omega Ldt, Manchester, UK, 2002.
20. *Quel Thermocouple Choisir?*, Thermocoax S.A., Lyon, 2002, pp. 2–31.
21. F. Medjedoub: Ph.D. Thesis, École des Mines d'Albi-Carmaux, Albi, France, 2004, pp. 27–30.
22. V. Camille, V. Florian, A. Hamasaiid, and G. Dour: Report Project ANCC, EMAC, Albi, France, 2006.
23. G. Fortin, P.R. Louchez, and F.H. Samuel: *Rev. Metall./Cah. Inf. Technol*., 1994, vol. 9 (5), pp. 771–80.
24. J. Issac, G.P. Reddy, and G.K. Sharma.: *Br. Foundryman*, 1985, pp. 465–68.
25. M. Bamberger, B.Z. Weiss, and M.M. Stuple:: *Mater. Sci. Technol*., 1987, vol. 3, pp. 49–56.
26. F. Michel, P.R. Louchez, and F.H. Samuel: *AFS Trans*., 1995, vol. 103, pp. 275–83.
27. T.-G. Kim and Z.-H. Lee: *Int. J. Heat Mass Transfer*, 1997, vol. 40 (15), pp. 3513–25.

28. K.N. Parbhu and W.D. Griffith: *J. Mater. Sci. Technol*., 2002, vol. 18 (7), pp. 804–10.
29. S. Wei, J. Dillingham, M.R. Jiranek, K. Nyamekye, C.W. Ramsay, D.R. Askeland, and R. Pischel: *AFS Trans*., 1996, vol. 104, pp. 251–62.
30. J.C. Hwang, H.T. Chuang, S.H. Jong, and W.S. Hwang: *AFS Trans*., 1994, vol. 102, pp. 877–83.
31. G. Dour: *Fonderie-Aide-Mémoire*, 1st ed., Dunod, Paris, 2004, pp. 151–57.
32. F. Decultieux: Ph.D. Thesis, Ecole des Mines de Paris, Paris, 1996.
33. M. Prates and H. Biloni: *Metall. Trans*., 1972, vol. 3, pp. 1501–10.
34. I.F. Bainbridge: Ph.D. Thesis, University of Queensland, Queensland, Australia, 2005, pp. 128–35.